International Journal of Innovative
Computing, Information and Control
Volume 9, Number 6, June 2013

ICIC International ©2013 ISSN 1349-4198
pp. 2347–2360

DESIGN AND FLIGHT TEST OF A SMALL TRI-ROTOR UNMANNED VEHICLE WITH A LQR BASED ONBOARD ATTITUDE CONTROL SYSTEM

Sukhwan Yoon, Seung Jun Lee, Byoungjin Lee
Chang Joo Kim, Young Jae Lee and Sangkyung Sung

Department of Aerospace Information Engineering
Konkuk University
No. 1, Hwayang-dong, Gwangjin-gu, Seoul 143-701, South Korea
{sukhwan; sksung}@konkuk.ac.kr

Received March 2012; revised July 2012

Abstract. *This paper presents design and implementation of a tri-rotor UAV (unmanned aerial vehicle) system with single tilt dynamics on a tail rotor for the flight dynamic control. The analytic aerodynamic model of the suggested tri-rotor UAV is presented based on the force and moment equation and its parameters are calculated through an experiment. For the flight dynamics control, the equilibrium point is computed through a numerical analysis and based on it, the linearized model of the single tilt tri-rotor is developed. An optimal control law via the LQR method is applied for the attitude control of the UAV system and simulation results validated the performance under both linear and nonlinear models. Finally, the single tilt tri-rotor system is manufactured and onboard avionics are implemented using a small-sized AHRS (attitude and heading reference system) and real-time processor module. Flight tests demonstrated that the designed attitude controller operates successfully with a fast yaw motion control performance.*
Keywords: Tri-rotor UAV, Single tilt dynamics, Attitude control, LQR, Yaw motion control

1. **Introduction.** Various types of UAVs (Unmanned Aerial Vehicles) have been developed to perform a required mission in dangerous and human-prohibited environments. Among many unmanned systems, UAVs have the most complicated mechanism in their implementation owing to the increased DOF (degree of freedom) and difficulty in stability control of the flight dynamics. Accordingly, many challenges exist for the feedback controller design. Yet in turn, they provide wider application including military mission and public rescue service as well as civil applications. Monitoring tall buildings and electric power towers, investigating monuments, and rescuing service over indoor or outdoor simultaneously are those examples [1]. One of the recent trends about UAV is to develop a small sized VTOL (Vertical Take Off and Landing) UAV for both indoor and outdoor applications. Due to spot take-off and landing functionality, it can achieve a reconnaissance flight mission where a very narrow and blind spot is only allowed, together with a hovering capability [2,3].

Roughly, VTOL UAV can be divided into a general helicopter and multi rotor UAV. Among various multi rotor systems, a quad-rotor UAV has two paired rotors facing to each other, which can remove the inverse torque effectively. Besides, as there is no swash plate, its structure is simple and easy to repair [2]. From a dynamic model viewpoint, the quad-rotor UAV has a simpler dynamic equation than that of non-symmetric multi-rotor UAV or the tilt rotor UAV systems. This comes from the dissymmetry between employed rotor moments or partitioned thrusts due to titled rotor axes. Especially, as

the tilt rotor system induces axis divided force elements from the same rotor thrust, the resulting motion caused by these collective forces is highly coupled. This resulted in a more complicated controller output design for maneuvering command compared with quad-rotor system that only adjusts the angular speed of the paired rotors to trigger motion command.

Due to the above UAV features, many studies have been done to investigate dynamic characteristics and control of multi rotor UAV systems. As a result, much progress on auto pilot system is achieved with the help of modern control theory and sensor fusion, supported by experimental demonstrations. For instance, a vision sensor aided navigation system is designed for the robust stability control of the quad rotor system using the derived aerodynamic model and integrated navigation data [1]. From the aspect of controller design, fuzzy control, hybrid feedback linearization control, adaptive sliding mode and robust nonlinear control methods are taken in various complex vehicle dynamic models [5]. Particularly for multi rotor UAV system, both a linear controller such as PID and a nonlinear controller such as the sliding mode, and the backstepping control mechanism are employed for vehicle's attitude control [8-10]. Flight test result further verified the performance of the adapted control schemes. Meanwhile, the extended parameter estimation is attempted by using external navigation sensors for outdoor application of a small sized quad rotor UAV [10].

Despite simple dynamic model and control logic design, there exist some disadvantages in quad rotor UAV system. First, it requires more motors and blades than a normal helicopter, which increases implementation complexity and energy consumption rate. For simple control logic design, a strong requirement on the frame symmetry should be assumed. Especially, yaw maneuvering is just governed by the torque induced by the angular momentum difference between the paired rotors; thus a transient response is relatively slow. To enhance the implementation and maneuverability features, recent researches have introduced varied multi rotor design including a tilt angle rotor and coaxial multi-rotor for the better performance [3,4,11].

Reviewed from the previous studies, the multi-rotor UAV employing an additional tilt motion has the following characteristics. In consideration of a multi-rotor design without symmetry constraint, the UAV frame configuration is relatively free. Moreover, together with tilting subsystem, the shape design can be further extended to satisfy fast maneuvering missions. As reported in [11], a typical tilting mechanism on each rotor may greatly increase the maneurability in yawing and other axis simultaneously, yet its dynamic model becomes undesirably complicated. On the other hand, coaxial design can internally cancel the anti-torque elements, yet implementation burden increases as it requires a doubly complicated rotor system. Thus, considering a simple implementation without the complete symmetry condition and the capability of quick maneuvering through the tilting dynamics, this paper focuses on the tri-rotor UAV system with single tilt dynamics in tail rotor and its control system design.

In view of tri-rotor's dynamics and controller design, the tilt motion in tail rotor inherently causes a separation of thrust into two components, which serve as a lift force and anti torque, respectively. The main advantage of this approach is that the motivated anti-torque triggers a swift response on the yawing motion while the tilt angle and the RPM change together stabilize the attitude of UAV body. Due to strict nonlinearities in moment and torque equations, the most typical controller for tilt tri-rotor can be designed via the Lyapunov based control logic [2-4]. Among the related studies, it is notable that a saturating function based sequential control strategy is taken to cover the physical limitation on actuator dynamics [4]. Despite its nonlinear controller design considering input limitation, the reported work only verified the control performance of

attitude stabilization in a static hovering case. This results from a control law design ensuring a local stability around the equilibrium, which typically lacks for considering the transient response of the closed loop system. Similar work in [2] included experimental results of simple transient response with additionally burdensome state observer design, yet it demonstrated the nonlinear control law provided a relatively poor performance in attitude stabilization.

In this paper, as a comparable extension of the preliminary studies, a single tilt tri-rotor system is manufactured and tested with the embedded real time control logics. For control system design, a simple and straightforward approach is taken based on a conventional optimal state feedback controller design. Owing to its design flexibility, closed loop design was easily tuned and the transient response performance for attitude stabilization was demonstrated successfully through experiments. Additionally, the adopted virtual instrumentation platform and remote control scheme was turned out to be very efficient in realizing real time flight dynamics control and performance evaluation.

This paper is organized as follows. First, the nonlinear dynamic model is derived using the force and moment equations in Section 2; an optimal controller design and simulation based on the linearized model is studied in Section 3; then a testbed tri-rotor plant is manufactured and flight test is done by implementing the realtime controller and sensor module onboard UAV in Section 4; finally, conclusion is made in Section 5.

2. **Single Tilted Tri-rotor UAV.** The schematic of the proposed single tilted tri-rotor UAV system is presented in Figure 1.

Three main rotors of the tri-rotor UAV system are represented by Rotor 1, Rotor 2, and Rotor 3 as in the figure, which take a role of main thrust for flight. The tail side, i.e., Rotor 3 has an x-axis tilting motion that causes an inverse torque in the counterclockwise direction of z-axis. Note that simple tilt motions at Rotor 3 cause both yaw and pitch moment at the same time. This is in contrast to a general quad-rotor UAV, where yawing moment is generated by moment difference from two rotor pairs and pitch moment by thrust difference between rotors within a pair. As each moment difference is originated from angular speed of each rotor, the bandwidth of control system primarily depends on the transient response of motor speed control. Comparatively, the transient response of the adopted tri-rotor depends on the titling motion dynamics, which provides faster response than rotor speed dynamics.

The following equations represent tri-rotor's aerodynamic model in terms of force and moment, respectively. In the modeling, it is assumed that tilting moment caused by tail

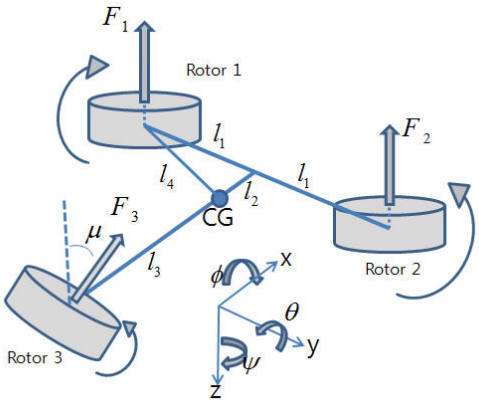

FIGURE 1. Single tilted tri-rotor UAV

rotor is neglected; translational force is proportional to angular velocity of rotor; the dynamics from torque to angular velocity of rotor is negligible; the drag of blade at the rotor 3 only affects the yawing moments.

$$F_x = m(\dot{u} - vr + wq) + mg\sin\theta \tag{1}$$

$$F_y = m(\dot{v} - ru + pw) - mg\sin\phi\cos\theta \tag{2}$$

$$F_z = m(\dot{w} + pv - qr) - mg\cos\phi\cos\theta \tag{3}$$

$$L = I_{xx}\dot{p} - I_{xz}\dot{r} - I_{xz}pq + (I_{zz} - I_{yy})qr \tag{4}$$

$$M = I_{yy}\dot{q} + (I_{xx} - I_{zz})pr + I_{xz}(p^2 - r^2) \tag{5}$$

$$N = I_{zz}\dot{r} - I_{xz}\dot{p} + (I_{yy} - I_{xx})pq + I_{xz}qr \tag{6}$$

Here F_x, F_y, F_z are sum of external forces for each axis. L, M, N are the sum of moments acting on each axis and p, q, r are the angular velocity on each axis. u, v, w is velocity on each axis. ϕ, θ, ψ is angle of roll, pitch, and yaw.

Next, moments generated by three rotor's angular speed and tilt angle of Rotor 3 are represented by the driving thrust as shown below.

$$U_t = b_1\left(\Omega_1^2 + \Omega_2^2\right) + b_2\Omega_3^2\cos\mu \tag{7}$$

$$U_x = l_1 b_1\left(\Omega_1^2 - \Omega_2^2\right) \tag{8}$$

$$U_y = l_2 b_1\left(\Omega_1^2 + \Omega_2^2\right) - l_3 b_2\Omega_3^2\cos\mu \tag{9}$$

$$U_z = l_4 d_1\left(-\Omega_1^2 + \Omega_2^2\right) + l_3 d_3\Omega_3^2 + l_3 b_2\Omega_3^2\sin\mu \tag{10}$$

Here, U_t is the total thrust of UAV in the z-axis; U_x is the rolling moment in the x-axis(L), U_y is the pitching moment in the y-axis(M), U_z is the yawing moment in the z-axis(N). And b_1, b_2 is thrust coefficient; d_1, d_3 is drag coefficient; Ω_1, Ω_2, Ω_3 is RPM of each rotor and μ is tilt angle.

Figure 2 represents a tilting system geometry of the Rotor 3. The tilt motion enables the roll movement and the inclination angle μ on z-axis separates force components into y and z axis.

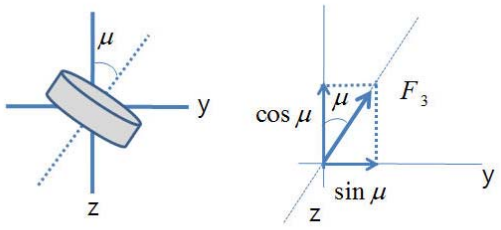

FIGURE 2. Coordinate and geometry of tilt system model

TABLE 1. Physical parameters

Parameter	*Value (unit)*	*Parameter*	*Value (unit)*
I_{xx}	$5.7211e^{-3}$ (kgm^2)	l_2	0.122 (m)
I_{yy}	$7.3933e^{-3}$ (kgm^2)	l_3	0.23 (m)
I_{zz}	$1.2545e^{-2}$ (kgm^2)	l_4	0.225 (m)
I_{xz}	$3.514e^{-3}$ (kgm^2)	b	$1.3678e^{-4}(Ns^2)$
l_1	0.19 (m)	d	$2.4323e^{-5}$ $(N\text{ms}^2)$

In Table 1 I_{xx}, I_{yy}, I_{zz} are moment of inertia of each body frame axis, respectively. l_1, l_2, l_3, l_4 are moment arm length from center of gravity point. b is the thrust coefficient and d is the drag coefficient on blade. I_{xz} is a coupled inertia moment.

Using the derived force and moment equation, the dynamic model of the tilted tri-rotor UAV can be given by a state space model as below

$$\dot{x} = f(x, u) \tag{11}$$

where the state variable and control input are depicted by

$$x = \begin{bmatrix} \phi & \dot{\phi} & \theta & \dot{\theta} & \psi & \dot{\psi} \end{bmatrix}^T \tag{12}$$

$$u = \begin{bmatrix} \Omega_1 & \Omega_2 & \Omega_3 & \mu \end{bmatrix}^T \tag{13}$$

Note that the state variables are defined in the body coordinate frame (B-frame). This enables straightforward computation for control input since the measured angular rate from the sensor is given in the body frame. Thus B-frame is adopted for the simplicity of attitude controller design and application to experiments. In this scheme, the nonlinear model for tri-rotor attitude dynamics is represented by the following equation.

$$\begin{bmatrix} \dot{\phi} \\ \dot{\theta} \\ \dot{\psi} \end{bmatrix} = \begin{bmatrix} \left(\frac{I_{yy}-I_{zz}}{I_{xx}}\right) x_4 x_6 + \frac{I_{xz}}{I_{xx}} x_6 + \frac{I_{xz}}{I_{xx}} x_2 x_4 + \frac{U_x}{I_{xx}} \\ \left(\frac{I_{zz}-I_{xx}}{I_{yy}}\right) x_2 x_6 + \frac{I_{xz}}{I_{yy}} (x_6^2 - x_2^2) + \frac{U_y}{I_{yy}} \\ \left(\frac{I_{xx}-I_{yy}}{I_{zz}}\right) x_2 x_4 + \frac{I_{xz}}{I_{zz}} x_4 x_6 + \frac{U_z}{I_{zz}} \end{bmatrix} \tag{14}$$

3. **Controller Design and Simulation.**

3.1. **Linearization and LQR controller design.** To design a linear controller for attitude stabilization, a perturbation model is assumed on the UAV dynamics. During a linearization process, a small angle terms are employed to generate error state as $\delta x := x - x_e$ and the corresponding input as $\delta u := u - u_e$. The nominal trim point is computed by the *Newton – Raphson* method, which provides the following input condition for $x_e = 0$.

$$u_e = \begin{bmatrix} 8418 & 8418 & 8676 & 2.407 \end{bmatrix}^T \tag{15}$$

By applying the equilibrium in (15) with hovering state condition, the Jacobian operation generates a linearized model as follows:

$$\delta \dot{x} = A \times \delta x + B \times \delta u \tag{16}$$

$$A = \begin{bmatrix} 0 & 1 & 0 & 0 & 0 & 0 \\ 0 & 0 & 0 & 0 & 0 & \frac{I_{xz}}{I_{xx}} \\ 0 & 0 & 0 & 1 & 0 & 0 \\ 0 & 0 & 0 & 0 & 0 & 0 \\ 0 & 0 & 0 & 0 & 0 & 1 \\ 0 & \frac{I_{xz}}{I_{zz}} & 0 & 0 & 0 & 0 \end{bmatrix},$$

$$B = \begin{bmatrix} 0 & 0 & 0 & 0 \\ \frac{2l_1 b_1 \Omega_{1e}}{I_{xx}} & \frac{-2l_1 b_1 \Omega_{2e}}{I_{xx}} & 0 & 0 \\ 0 & 0 & 0 & 0 \\ \frac{2l_2 b_1 \Omega_{1e}}{I_{yy}} & \frac{2l_2 b_1 \Omega_{2e}}{I_{yy}} & \frac{-2l_3 b_2 K_c \Omega_{3e}}{I_{yy}} & \frac{l_3 b_2 K_s \Omega_{3e}^2}{I_{yy}} \\ 0 & 0 & 0 & 0 \\ \frac{-2l_4 d_1 \Omega_{1e}}{I_{zz}} & \frac{2l_4 d_1 \Omega_{2e}}{I_{zz}} & \frac{2l_3 d_3 \Omega_{3e} - 2l_3 b_2 K_s \Omega_{3e}}{I_{zz}} & \frac{l_3 b_2 K_c \Omega_{3e}^2}{I_{zz}} \end{bmatrix} \tag{17}$$

where K_c, K_s represents $\cos(\mu e)$ and $-\sin(\mu e)$, respectively.

Given the linear model by A and B, a general full state feedback linear quadratic regulator is employed for the attitude control. In controller design, the optimal control performance index in (18) is used with infinite integration period,

$$J = \int_0^\infty \left(x^T Q x + u^T R u\right) dt \tag{18}$$

where control input $u = -Kx = -R^{-1}B^T P x$ is achieved to get the minimized index function via a full state feedback. Following the conventional LQR controller design procedure, the steady state optimal gain is calculated by solving the matrix Riccati equation as below,

$$A^T P + PA - PBR^{-1}B^T P + Q = 0 \tag{19}$$

In solving P from the Riccati equation, the weight matrix, Q and R are adapted, which can tune the regulating strength of state and input, respectively. In tri-rotor system, with the chosen Q and R in (20), the final feedback gain is expressed by (21). The weight matrices are adjusted such that control input regulates roll, pitch and yaw angles faster than angular rate. Also a tradeoff between transient response and control input boundedness is considered for the weight selection.

$$Q = diag[\ 1000 \quad 10 \quad 1000 \quad 10 \quad 1000 \quad 10\ ], \quad R = I_{4\times 4} \tag{20}$$

$$K = \begin{bmatrix} 22.2813 & 4.7303 & 13.0868 & 2.9802 & -2.3826 & -0.2036 \\ -22.3426 & -4.7460 & 13.1864 & 2.9926 & 0.5670 & -0.2170 \\ 0.0595 & 0.0153 & -25.4971 & -5.7964 & 1.7619 & 0.4082 \\ 2.0856 & 0.3331 & 2.1801 & 0.2226 & 31.4785 & 3.3407 \end{bmatrix} \tag{21}$$

3.2. **Simulation and discussion.** In LQR simulation, the designed feedback controller based on the linearized model is verified by applying it to both the original nonlinear and the linearized plant model for comparison. In each case, an external disturbance is applied through an intentional variation in rotor's angular speed. Variation of the thrust due to the rotor speed change is equivalent with an external disturbance. Attitude response is observed to validate system performance. To verify the linearized model and controller tolerance near the equilibrium, the simulation result using the same LQR gain K is compared for both cases. Simulation scenario contains initial hovering response and the response with a disturbance applied to the hovering state afterwards. Note that the initial condition for the nonlinear model is set to (15), which is the same as the case of linear model.

Simulation 1: Hovering case

Figure 3 shows the results of the hovering simulation for linear and nonlinear model, respectively. In the linear model result, attitude angle and rate are observed to maintain zero state. In nonlinear model case, the attitude angle is observed to saturate into slightly deviated value from zero, while rate quickly converge to zero. This mainly results from controller design process using the approximated plant and trim point accuracy. Yet, considering system's tolerance, the result reveals the basic performance of the controller.

Simulation 2: 300rpm pulse input on Rotor 1

The designed attitude control law is further verified by applying an external force on Rotor 1. This is realized by applying an equivalent electric force caused by the change of rotor RPM from the nominal status. In many practical cases, electrical excitations are widely used for the accurate measurement of dynamic response such as step response. Figure 4 shows simulation results when the pulse input of 5 cycles/sec is intentionally applied to the Rotor 1. In both results, the last subfigure shows the applied rpm curve

at Rotor 1. Note that the nominal rotor speed at equilibrium is 140 cycles/sec. The rpm change of pulse input is applied at 2 sec and stopped at 4 sec. When the external disturbance is applied at 2 sec, roll and pitch angle changes with the positive direction as U_x and U_y increase due to Ω_1. On the other hand, yaw angle changes with the negative direction as U_z decreases due to Ω_1. With a proper stabilizing controller, it is observed that the rate converges to zero quickly in both cases, although negligible performance difference is observed during the transient response period in falling time and settling time.

Simulation 3: Altitude control during hovering status

In addition to attitude control, altitude control is further investigated. For the altitude control, the state variables are augmented to include position state. Using force equation in (1) $\sim$ (3), the state transition matrix and input matrix in a linearized form is represented by (22), respectively. Submatrices are derived as (23) considering the extended state variables. Note that $A22$ equals A. Note that the extended state variables are all represented in body frame for the computation convenience, yet the position data can be further transformed into local navigation frame for physical understanding.

$$\bar{A} = \begin{bmatrix} A_{11} & M & A_{12} \\ L & L & L \\ 0_{6\times 6} & M & A_{22} \end{bmatrix} \quad \bar{B} = \begin{bmatrix} B_{11} \\ B_{21} \end{bmatrix} \tag{22}$$

where

$$A_{11} = \begin{bmatrix} 0 & 0 & 0 & 1 & 0 & 0 \\ 0 & 0 & 0 & 0 & 1 & 0 \\ 0 & 0 & 0 & 0 & 0 & 1 \\ 0 & 0 & 0 & 0 & 0 & 0 \\ 0 & 0 & 0 & 0 & 0 & 0 \\ 0 & 0 & 0 & 0 & 0 & 0 \end{bmatrix} \quad A_{12} = \begin{bmatrix} 0 & 0 & 0 & 0 & 0 & 0 \\ 0 & 0 & 0 & 0 & 0 & 0 \\ 0 & 0 & 0 & 0 & 0 & 0 \\ 0 & -g & 0 & 0 & 0 & 0 \\ g & 0 & 0 & 0 & 0 & 0 \\ -g & -g & 0 & 0 & 0 & 0 \end{bmatrix}$$

$$B_{11} = \begin{bmatrix} 0 & 0 & 0 & 0 \\ 0 & 0 & 0 & 0 \\ 0 & 0 & 0 & 0 \\ 0 & 0 & 0 & 0 \\ 0 & 0 & \frac{K_s}{m} & \frac{T_3 K_c}{m} \\ -\frac{1}{m} & -\frac{1}{m} & -\frac{K_c}{m} & \frac{T_3 K_s}{m} \end{bmatrix} \quad B_{21} = B \tag{23}$$

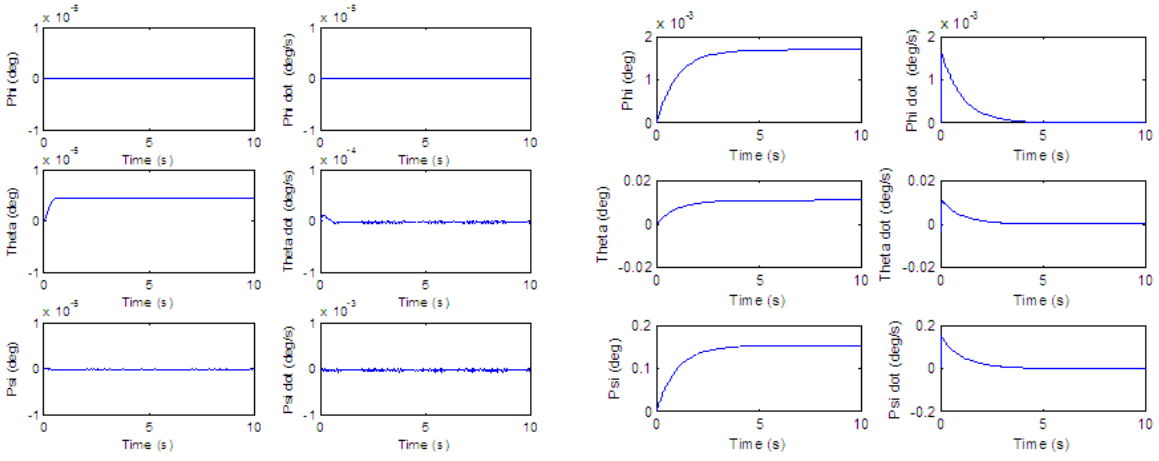

FIGURE 3. Hovering simulation result: linear vs. nonlinear model

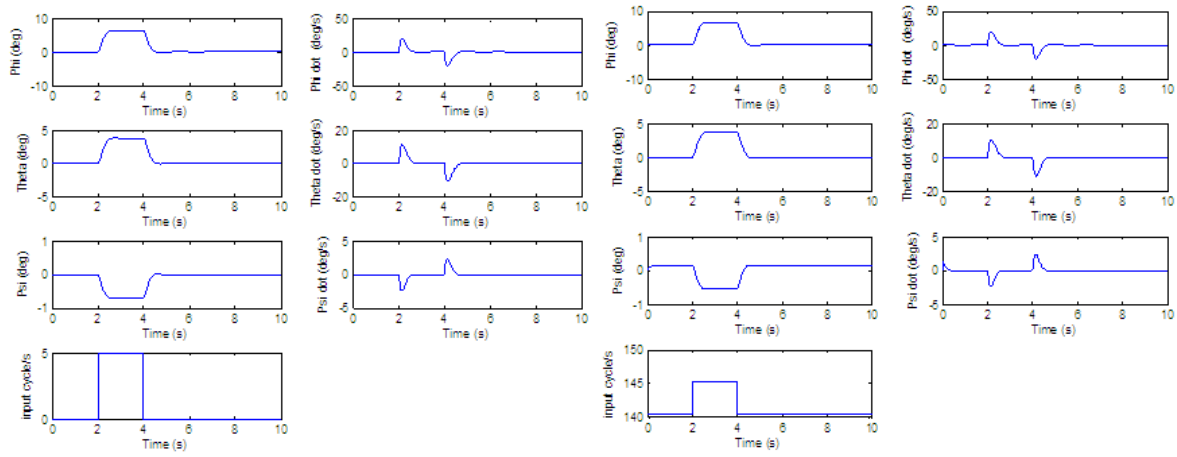

FIGURE 4. Pulse input simulation result: linear (left) vs. nonlinear (right) model

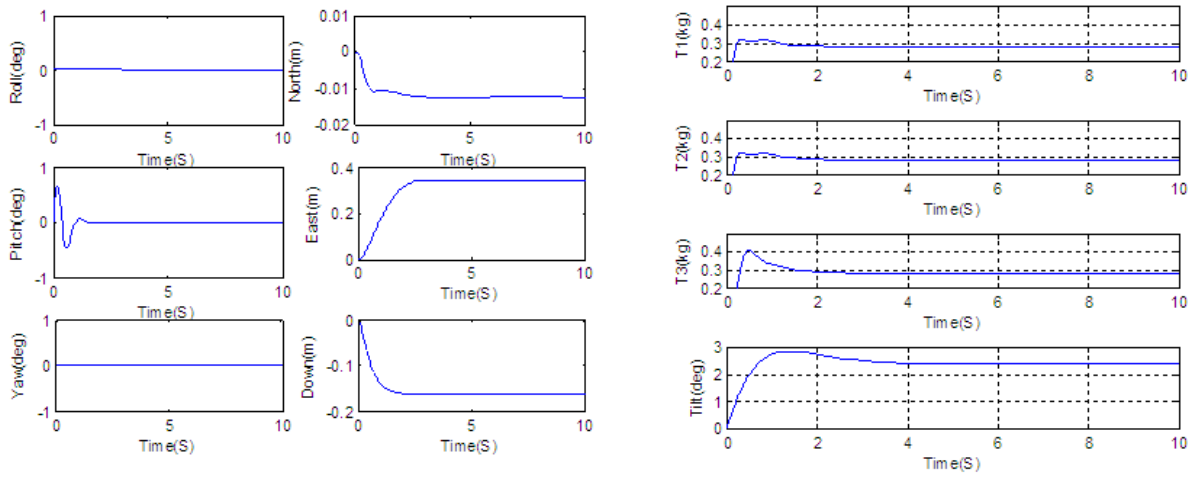

FIGURE 5. Altitude control result (attitude in B-frame and position in N-frame)

Repeating the LQR approach, the computed gain is computed as (24).

$$K = \begin{bmatrix} -3.9781 & 2.7474 & -1.8434 & -6.3275 & 2.4307 & -1.7703 & 2.8338 & 49.6790 & 17.4921 & 2.4982 & 18.2122 & 84.0472 \\ -3.9781 & -2.9227 & -1.4675 & -6.3150 & -2.6441 & -1.4202 & 1.2610 & 49.2732 & -19.2169 & -2.4821 & 18.2356 & -92.1797 \\ 4.2843 & -0.0725 & -3.0724 & 6.8177 & -0.1280 & -2.9659 & 4.2433 & -49.9158 & -1.8708 & 0.0155 & -19.1590 & -8.8806 \\ -0.0658 & 5.8227 & 0.0950 & -0.1070 & 5.1998 & 0.1347 & 28.2435 & 0.1956 & -17.9232 & 0.0376 & 0.1924 & -85.9613 \end{bmatrix} \tag{24}$$

Figure 5 left shows the simulation result of attitude and position when the vehicle is controlled to keep hovering at 0.16 meter above the nominal altitude. Starting from the trim point, simulation result verifies that attitude control is achieved with a similar transient response as hovering only case. In the figure, it is observed the altitude is regulated stably at the target height of 0.16m with 1.8 sec rising time. Figure 5 right shows thrust converted into weight and tilt angle during the altitude control. It is clear that the thrust requires higher power during the transient period. Outstandingly, rotor 3 reaches large thrust overshoot during tilt transient motion, which exceeds the designed 100g load. This puts an experimental constraint in practice because the payload margin of UAV is insufficient.

4. Flight Experimental Result.

4.1. H/W implementation.

In this section, hardware implementation and attitude control experiment is presented. The testbed tri-rotor is manufactured with one of rotors equipped with a tilting motion function. Each rotor with blade size of 7 inches is protected by the guard ring for safety. Total weight is about 840g including onboard controller, battery, and guard ring. In the center of UAV, main electronics modules are installed with the flight control computer (FCC) and onboard attitude and heading reference system (AHRS). The embedded FCC is implemented with ATmega128 having an operation clock of 16-MHz. The employed AHRS is a small size inertial measurement unit (IMU), MI-3300, that can provide attitude and rate data of 3 axes with the update rate of 100 Hz. For the power train components, a DC brushless motor that can output up to 9500 rpm was used. Installed with the 7-inch blade, each motor can lift up to about 300g. In real experiment, we only focused on attitude control of the single tilt tri-rotor UAV. This because our primary interest was to verify the effectiveness of tilt rotor for yaw motion control, simultaneously with roll and pitch stabilization. Besides, in our manufactured vehicle, the total thrust of vehicle was 900g, with a thrust margin of 60g only. As demonstrated in Section 3, the controller requires thrusts exceeding the margin, thus altitude control experiment is not performed. Yet, to remove tension from hanging cord, rotor RPM is slowly increased such that the vehicle is slightly lifted from the initially suspended point.

Figure 6 presents the block diagram showing the experimental setup and data signaling flow of the tri-rotor UAV. In our experiment, the controller is realized in the remote control center. A typical RS232C serial communication is used for the data exchange between tri-rotor and control center. Controller implemented in the ground control center computes and outputs digital signal of PWM duty ratio by processing high rate IMU data. Then the duty ratio is transmitted to the onboard AVR, which converts it into a PWM signal for motor speed and tilt control.

In real implementation, the IMU data rate and output update rate from controller is set to 100 Hz and 50 Hz, respectively. However, the computational capacity of the onboard microcontroller was limited in executing this data processing in real time manner. Instead, a remote controller scheme is adopted. The possible problem in this scheme may be a control delay due to a communication latency time. In our case, the PWM signal is set to have 2 ms periods with output frequency of 50 Hz for rotor control. Thus the maximum allowed latency between consecutive PWM signal is about 18msec. Considering

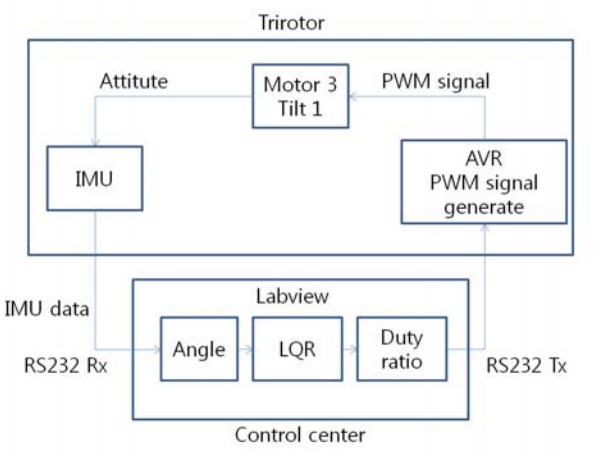

FIGURE 6. Hardware configuration for tri-rotor experimental

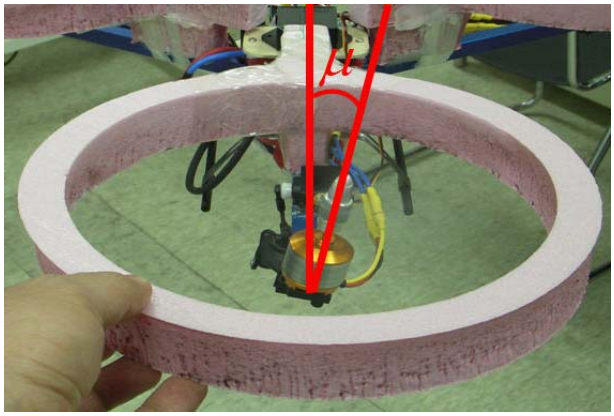

FIGURE 7. Tilt system on Rotor 3 with inclination angle applied for control

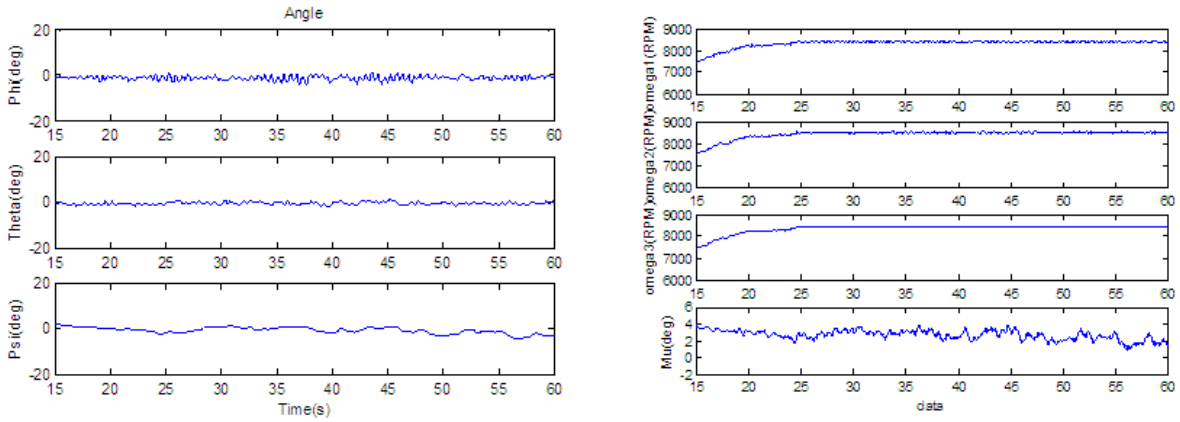

FIGURE 8. Hovering control result: attitude, RPMs, and tilt angle

the band rate of serial communication of 14400 Byte/sec, sensor rate of 4200 Byte/sec(42 Byte/packet, 100 Hz), and PWM output rate of 600 Byte/sec(12 Byte/PWM, 50 Hz), the occupancy ratio is just one third of the total band rate, thus resulted in negligible communication latency in practice. Furthermore, control design based on the virtual instrumentation via Labview in the remote computer greatly enhanced flexibility with real time gain tuning and monitoring.

Figure 7 explains the tilt system on the Rotor 3. Tilt system is mainly operated during suppressing the inverse torque and UAV heading control. Regardless of the installation angle of Rotor 1 and 2 from center line, their differential torque is automatically removed only if the symmetry is kept. Thus in our design, the tilt angle in Rotor 3 contributes to reject the self-generated torque and simultaneously the perpendicular lift force matching with other rotor's lift force. In Figure 7, an external human force to the clockwise direction is applied to the tri-rotor UAV in the hovering state, which generates a resisting torque to the counterclockwise direction by causing tilt motion.

4.2. **Flight test result.** The following shows various experiments to verify the designed control system performance. They consist of results from hovering test, hovering test under external disturbance, and yaw test.

Test 1: Hovering test

First, Figure 8 shows the result of hovering experiment. Despite a slight drift and fluctuations due to the unbalanced center of mass and sensor output drift, roll, pitch and yaw angle are measured to remain around the equilibrium. In the right figure, it can be

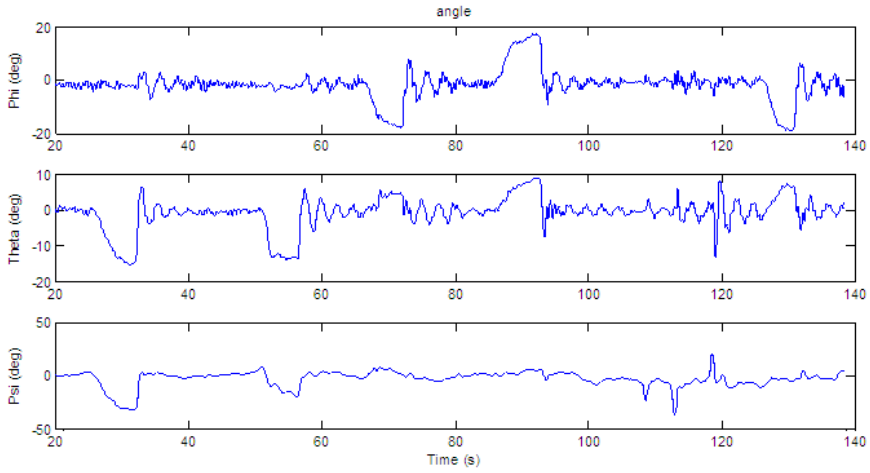

FIGURE 9. Roll and pitch control under external forces

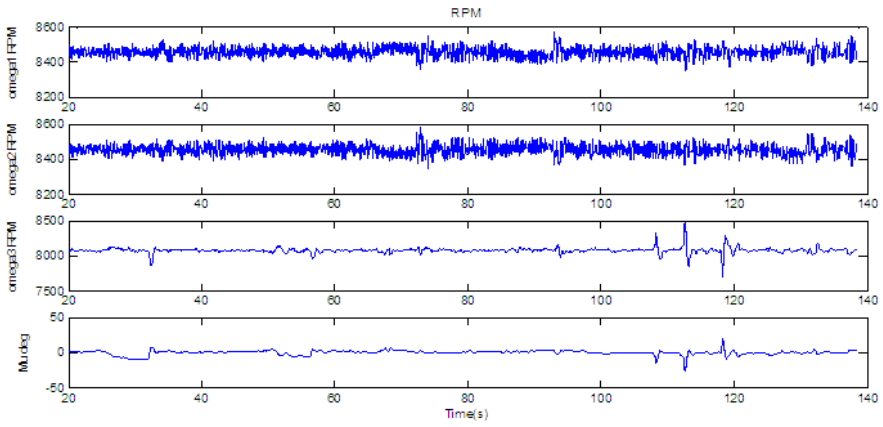

FIGURE 10. RPM control under external forces

further observed that the rotor speed of roll/pitch and yaw converges to around 8400 rpm and 8460 rpm, respectively, which is similar to the simulation result. Hovering state is best observed at periods of $25 \sim 45$ sec and the resulting tilt angle is measured as 2.45 deg on average. A slight yaw drift is detected after 45 sec, which is affected by the slowly rotating vehicle motion and attitude sensor's output drift.

Test 2: Attitude control with the manual external force

Figures 9 and 10 show the results of attitude control of tri-rotor UAV when the external disturbance is manually applied. Even after it is affected by the external forces, the attitude control system quickly recovers its hovering state within several seconds. In the figure, it is clearly observed that the disturbance causing pitch and roll motion between 15 and 20 deg are effectively regulated and continue a stable attitude. Although results at 30 sec and 55 sec provide regulation with a coupled dynamics between pitch and yaw axis, it is proved to have negligible coupling when observing response around 90 sec. The reason for a concurrent coupled dynamic response comes from the manual excitation of vehicle to an arbitrary direction. On the other hand, much larger angle deviation in yaw axis via external disturbance can be controlled, since it does not change roll and pitch stability condition significantly. In the figure, angle deviation of about 35 deg is applied in yaw axis via external disturbance input, yet it returns to the initial heading angle of the hovering state immediately without any unstable roll and pitch attitude. This can

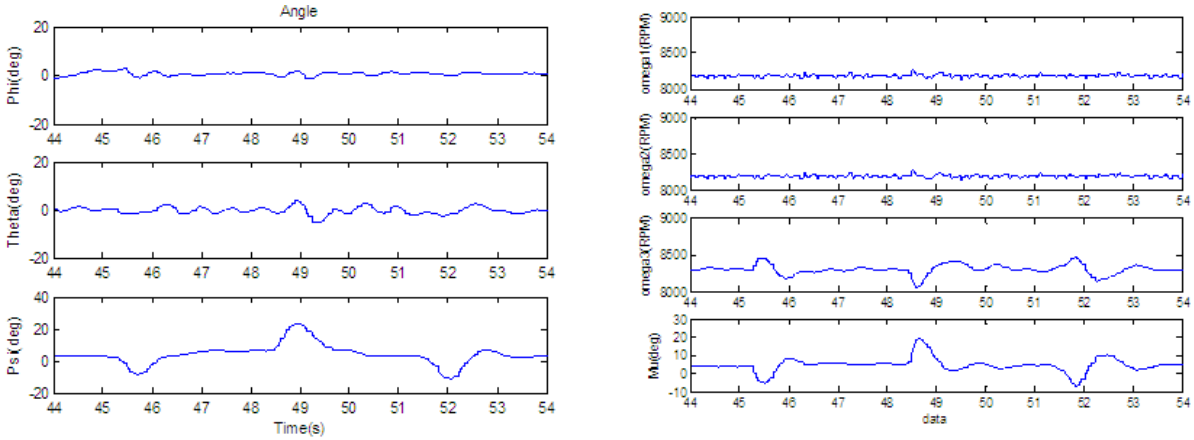

FIGURE 11. Yaw control result with rpm and tilt angle change

confirm that the coupling effect between axes is negligible. Besides, as there is no position control loop, when controller changes rotor's rpm, the tri-rotor UAV tends to slide in the horizontal plane via thrust change and the position is not maintained at a fixed place.

Test 3: Yaw control using tilt motion under manual disturbance

To show the characteristic control performance of the tilt tri-rotor UAV system, experimental result of yawing motion control is observed in detail. Figure 11 left provides the attitude angle and control input signal, respectively. Three disturbances, during 45 sec, 48 sec and 51 sec intervals, are exerted into the yaw direction with a small effect on other axes too. During three trials, heading deviation between 10 and 15 deg appears. Both figures in Figure 11 shows a fast response of yaw control with about 0.5 sec rising time. During disturbance intervals, tilt system on the Rotor 3 operates to change the tilt angle and the rpm of Rotor 3 also changes to maintain hovering attitude. Figure 11 left illustrates that the first disturbance causes negative yaw angle initially and to control this angle (refer to Figure 2 and Figure 11 right), tilt system generates a negative tilt angle and separates force to yield a negative component in y-axis. This force component to the minus y-axis brings on a positive yaw angle such that the UAV maintains hovering state. Compared with typical quad-rotor UAV dynamics, the obtained results show an improved response time and maneuverability as desired.

Finally, Figure 12 shows the yaw recovery result after an external disturbance is manually applied through a stick. In the upper picture, as the stick continues to rotate vehicle into the counterclockwise direction with the angle deviation(ψ), the Rotor 3 shows an apparent negative tilt angle to resist the applied disturbance. The lower picture shows tilt system when external disturbance is removed and the tri-rotor UAV precisely returns to its initial posture. The tilt angle continues the trim point angle stably.

5. **Conclusions.** In this paper, a single tilt tri-rotor UAV system is presented to highlight some advantages over the typical quad-rotor UAV system. First the aerodynamic force and moment equations are derived, as well as control moment equation. For the controller design, a model linearization is applied, and the resulting linear optimal controller is investigated. Simulation studies verified the adaptability of the designed LQR controller to the nonlinear plant model. For experiment, a single tilt tri-rotor system is manufactured and the partially onboard flight control system is implemented. In the experiment, a remote control station provides control input in the form of duty ratio through a serial communication. Disturbance test during hovering status demonstrated the validity of the

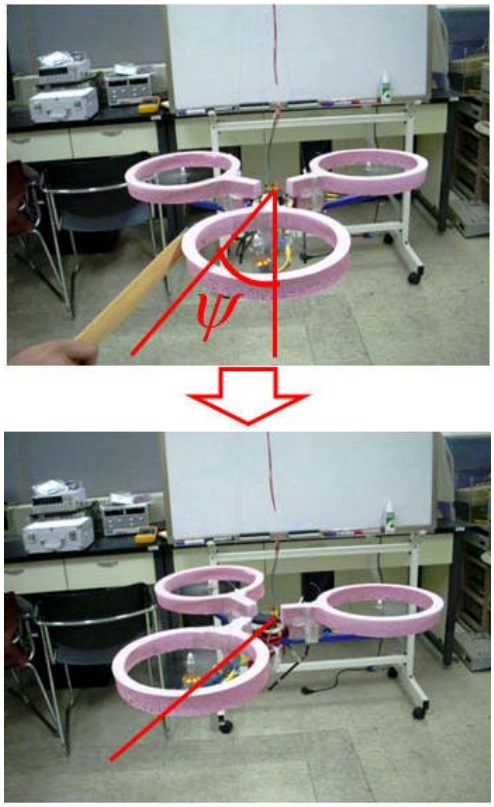

FIGURE 12. Yaw control result: heading recovery after external disturbance

designed controller and derived dynamic model. Further research includes a nonlinear controller design and its verification via flight test.

Acknowledgment. This work was supported by the Faculty Research Fund of Konkuk University in 2012.

REFERENCES

[1] D.-Y. Won, *Dynamic Modeling and Control System Desing for a Quad-Rotor UAV*, Master Thesis, KAIST, 2007.

[2] S. Salazar-Cruz, R. Lozano and J. Escareno, Stabilization and nonlinear control for a novel trirotor mini-aircraft, *Control Engineering Practice*, vol.17, no.8, pp.886-894, 2009.

[3] J. Escareno, A. Sanchez, O. Garcia and R. Lozano, Triple tilting rotor mini-UAV: Modelilng and embedded control of the attitude, *Proc. of American Control Conference*, pp.3476-3481, 2008.

[4] S. Salazar-Cruz, F. Kendoul, R. Lozano and I. Fantoni, Real-time stabilization of a small three-rotor aircraft, *IEEE Transactions on Aerospace and Electronic Systems*, vol.44, no.2, pp.783-794, 2008.

[5] M. Oya, R. Okura, H. Shibata and K. Okumura, Robust control of vehicle active suspension systems, *ICIC Express Letters*, vol.6, no.4, pp.1019-1026, 2012.

[6] H. Rafaralahy, E. Richard, M Boutayeb and M. Zasadzinski, Simultaneous observer based sensor diagnosis and speed estimation of unmanned aerial vehicle, *Proc. of the 47th IEEE Conference on Decision and Control*, 2008.

[7] C. Wang, Y. Li, B. Xi and G. Yi, Modeling, control and flight testing for a saucer ducted fan UAV, *Proc. of the 3rd International Symposium on System and Control in Aeronautics and Astronautics*, pp.930-935, 2010.

[8] S. Bouabdallh and R. Siegwart, Backstepping and sliding-mode techniques applied to an indoor micro quadrotor, *Proc. of IEEE International Conference on Robotics and Automation*, pp.2247-2252, 2005.

[9] S. Bouabdallah, *Design and Control of Quadrotors with Application to Autonomous Flying*, Ph.D. Thesis, Lausanne Polytechnic University, 2007.

[10] A. Mokhtari and A. Benallegue, Dynamic feedback controller of euler angles and wind parameters estimation for a quadrotor unmanned aerial vehicle, *Proc. of IEEE International Conference on Robotics & Automation*, pp.2359-2366, 2004.

[11] D.-W. Yoo, H.-D. Oh, D.-Y. Won and M.-J. Tahk, Dynamic modeling and stabilization techniques for tri-rotor unmanned aerial vehicles, *International Journal of Aeronautical and Space Sciences*, vol.11, no.3, pp.167-174, 2010.